THE ASTROPHYSICAL JOURNAL, 455:108–124, 1995 December 10

THE CANADA-FRANCE REDSHIFT SURVEY. VI. EVOLUTION OF THE GALAXY LUMINOSITY FUNCTION TO $z \sim 1$

S. J. LILLY[1]
Department of Astronomy, University of Toronto, Toronto, Canada M5S 1A1
L. TRESSE[1] AND F. HAMMER[1]
DAEC, Observatoire de Paris–Meudon, 92195 Meudon, France
DAVID CRAMPTON[1]
Dominion Astrophysical Observatory, National Research Council of Canada, Victoria, Canada V8X 4MC
AND
O. LE FÈVRE[1]
DAEC, Observatoire de Paris–Meudon, 92195 Meudon, France
Received 1994 December 27; accepted 1995 June 19

ABSTRACT

The cosmic evolution of the field galaxy population has been studied out to a redshift of $z \sim 1$ using a sample of 730 I-band selected galaxies, of which 591 have secure redshifts with median $\langle z \rangle \sim 0.56$. The trivariate luminosity function $\phi(M, \text{color}, z)$ shows unambiguously that the population evolves and that this evolution is strongly differential with color and, less strongly, with luminosity. The luminosity function of red galaxies shows very little change in either number density or luminosity over the entire redshift range $0 < z < 1$. In contrast, the luminosity function of blue galaxies shows substantial evolution at redshifts $z > 0.5$. By $0.5 < z < 0.75$ the blue luminosity function appears to have uniformly brightened by approximately 1 mag. At higher redshifts, the evolution appears to saturate at the brightest magnitudes but continues at fainter levels, which leads to a steepening of the luminosity function. A significant excess of galaxies relative to the local luminosity function described by Loveday et al. in 1992 is seen at low redshifts $z < 0.2$ around $M_{AB}(B) \sim -18$, and these galaxies may possibly represent the descendants of the evolving blue population seen at higher redshifts. The changes seen in the luminosity function are also apparent in color-magnitude diagrams constructed at different epochs and in the V/V_{max} statistic computed as a function of spectral type. Finally, it is argued that the picture of galaxy evolution presented here is consistent with the very much smaller samples of field galaxies that have been selected in other wave bands and with the results of studies of galaxies selected on the basis of Mg II $\lambda 2799$ absorption.

Subject headings: cosmology: observations — galaxies: distances and redshifts — galaxies: luminosity function, mass function

1. INTRODUCTION

Deep redshift surveys, such as the Canada-France Redshift Survey (CFRS) described in earlier papers in this series (Lilly et al. 1995b, hereafter CFRS I; Le Fèvre et al. 1995, hereafter CFRS II; Lilly et al. 1995a, hereafter CFRS III; Hammer et al. 1995, hereafter CFRS IV; and Crampton et al. 1995, hereafter CFRS V), allow the direct study of galactic evolution with cosmic epoch. However, since different galaxies are observed at different epochs along the past light null-cone, the study of galaxy evolution is necessarily statistical in nature and requires a combination of knowledge about the population of galaxies at different epochs and an understanding of the physical processes occurring in individual galaxies, which together produce the changes seen in the population.

One of the most basic descriptions of the galaxy population is the luminosity function. This paper constructs the trivariate luminosity function of galaxies, $\phi(M, \text{color}, z)$, over the $0.0 < z < 1.3$ redshift interval from the CFRS sample described in CFRS I–CFRS V. We stress at the outset that this paper is concerned with describing the population of galaxies, defined at different epochs by various criteria, and no effort is made to determine the physical processes occurring in individual galaxies. Similarly, no assumptions are made, or conclusions drawn, as to whether individual galaxies move in or out of the various populations at different redshifts. We seek simply to provide a description of the luminosity function at each epoch.

H_0 is taken to be 50 km s^{-1} Mpc^{-1} throughout the paper, and, except where noted to the contrary, we generally assume $q_0 = 0.5$. Except where discussing the results of others, we have utilized the AB magnitude normalization scheme (Oke 1972), where $B_{AB} = B - 0.17$, $V_{AB} = V$, and $I_{AB} = I + 0.48$.

1.1. *Previous Work*

Until recently there have been very limited redshift data for field galaxies at cosmologically interesting redshifts. Early studies of the nature of the galaxy population at significant look-back times (e.g., Kron 1980; Koo 1986) were based on comparisons of color and magnitude distributions with the predictions of models, integrated over redshift space. With many free parameters available in the models, it was always possible to find acceptable fits to the data, and these models suffered from obvious problems of uniqueness.

[1] Visiting Astronomer, Canada-France-Hawaii Telescope, which is operated by the National Research Council of Canada, the Centre National de la Recherche Scientifique of France, and the University of Hawaii.

During the late 1980s, redshift data on limited samples of galaxies became available. In a landmark paper, Broadhurst, Ellis, & Shanks (1988) published a sample of 230 galaxies selected in the B band ($B < 21.5$) which had a median $\langle z \rangle \sim 0.2$. These data were initially analyzed as before in terms of comparing the $N(z)$ distribution with modeled predictions. This showed the initially surprising result that the $N(z)$ distribution appeared to be the same as that predicted for "no-evolution" models of the galaxy population despite the apparent excess in the $N(B)$ number counts relative to these same models. This result was extended to $21.5 < B < 22.5$ by Colless et al. (1990) (149 galaxies; $\langle z \rangle \sim 0.3$) and to $22.5 < B < 24$ by Cowie, Songaila, & Hu (1991) (12 objects with $\langle z \rangle \sim 0.4$—see also Lilly, Cowie, & Gardner 1991, hereafter LCG). Subsequently, Eales (1993) (see also Lonsdale & Chokshi 1993) constructed luminosity functions from the $B < 22.5$ samples and confirmed that they were consistent with a uniform increase in the apparent number density of galaxies.

If the faint end of the local galaxy luminosity function is flat, $\alpha \sim 1$, then an increase in the apparent number density requires, especially for higher q_0, either a dramatic luminosity evolution of some part of the galaxy population, a large degree of merging over relatively recent epochs, or a change in the cosmological geometry. All of these processes were invoked to varying degrees by various authors (e.g., LCG; Babul & Rees 1992; Cowie et al. 1991; Yoshii & Fukugita 1992; Broadhurst, Ellis, & Glazebrook 1992; see, for example, Lilly 1993 and Koo & Kron 1992 for recent reviews).

One significant problem with these relatively shallow samples is that the redshift baseline is sufficiently small that evolutionary effects can only be seen relative to the "local population," which places a premium on uniformity between the deep and local samples. Unfortunately, there are significant differences between the selection criteria for local determinations of the luminosity function and those based on deep surveys, and, as emphasized by Ferguson & McGaugh (1995), these can lead to differences in the derived luminosity function. Our new CFRS sample allows us to look for evolution within a single sample in which the selection criteria are essentially constant over a wide range of redshift.

Along with the I-band selected CFRS sample, smaller samples of faint galaxies selected at comparable depths in other wave bands are now becoming available. Glazebrook et al. (1995) have presented 84 objects with $22.5 < B < 24$ (analyzed to produce a luminosity function by Colless 1995), and Songaila et al. (1994) have a large sample of over 300 K-band selected galaxies spanning a very wide range of magnitudes that have been analyzed by Cowie, Songaila, & Hu (1995). However, in terms of galaxies at high redshifts, both of these samples are still quite small, each containing around 40–50 galaxies at $z > 0.5$ as against the 350 at $z > 0.5$ in the CFRS sample that is the subject of the present analysis (see § 1.3 below). We return to compare these different samples in § 4 below.

1.2. *The Importance of I-Band Selection*

As noted above, much of the initial work in this area has been based on B-selected samples of galaxies (Broadhurst et al. 1988; Colless et al. 1990; LCG; Cowie et al. 1991; Colless et al. 1993), with the goal of understanding the steep B-band galaxy counts, and has been generally confined to redshifts $z < 0.5$.

A basic difficulty encountered in B-selected samples at $z > 0.3$ is that the observed B band is redshifted progressively farther into the ultraviolet, where different types of galaxies have quite different properties. This is shown in Figure 1*a*, which shows the color difference between observed-B and rest-B for three galaxy spectral energy distributions from Coleman, Wu, & Weedman (1980, hereafter CWW). As can be seen in Figure 1*a*, the B-band k-corrections for different galaxy spectral types span 4 mag at $z \sim 0.75$. The large variation between different galaxy types has a number of undesirable consequences. First, predictions of what is expected, even in the simplest "no-evolution" scenario, depend sensitively on the assumed mix of galaxies as a function of absolute magnitude and the poorly constrained ultraviolet properties of each type of galaxy. This has led to a lingering controversy as to the amount of evolution required by these B-selected data (see, e.g., the discussions in Broadhurst et al. 1992; Lilly 1993; Koo & Kron 1992; Koo et al. 1993). As an extreme example, Koo, Gronwall, & Bruzual (1993) were able to match the counts and redshift distributions of the faint B-selected samples with a completely unevolving galaxy population by altering the properties of the local population (in essence assuming its properties are unknown) and assuming the most favorable cosmological geometry.

Similar difficulties are encountered in the more direct approach of computing luminosity functions. Clearly, the k-corrections for individual galaxies must be determined with considerable precision in B-selected samples. As described by Colless (1995), this can be reliably done from the observed $(B-R)$ colors, at least up to $z \sim 0.7$. A more subtle problem, however, is that the wide range of k-corrections within the population, or even within any reasonable subdivision by color, means that at a given observed B magnitude, different classes of objects will populate the rest B-band luminosity function at very different luminosities. Put another way, the faintest bins in absolute B magnitude (presumably produced at any redshift by the faintest galaxies at the survey limit) will

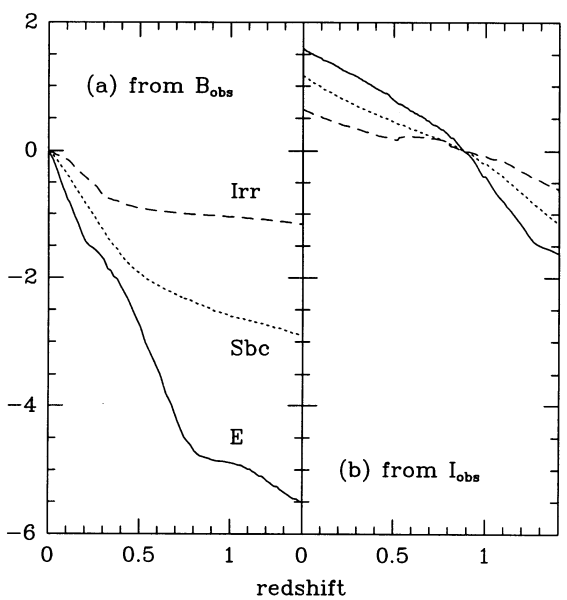

FIG. 1.—Values of the k-correction color (see text) required to produce absolute magnitudes in the rest B band from observations in the I band (*right-hand panel*) and B band (*left-hand panel*) as a function of redshift for three different spectral types of galaxies. Curves are for the CWW E spectral energy distribution (*top*), the CWW Sbc (*middle*), and CWW Irr (*bottom*).

contain only the bluest objects since the redder objects will have, at this same apparent B magnitude, a much brighter absolute B magnitude. The large range in k-corrections acts to effectively eliminate red objects from most of the luminosity function.

Selection in the I band substantially reduces the problems of working at high redshift ($0.3 < z < 1.0$). At $z \sim 0.5$ and at $z \sim 0.9$, the observed I band corresponds to the rest-frame V band and B band, respectively. Thus, the selection of the distant sample is as well matched as possible to that of most local samples of galaxies. Correspondingly, the k-corrections to produce a B-band luminosity function are minimal and do not depend strongly on spectral type (and not at all at $z = 0.89$). This is illustrated in Figure 1*b*, which shows the color between observed-I and rest-B for the three spectral energy distributions plotted in Figure 1*a*. Following from this, the mix of galaxy types at a given $M_{AB}(B)$ is not biased in terms of color.

1.3. *The CFRS Sample*

As an unprecedentedly large and deep I-band selected redshift survey, the CFRS is particularly well suited to the determination of the luminosity function at high redshift. In addition to the I-band selection, many aspects of the CFRS program were specifically designed with this goal in mind.

The statistically complete CFRS sample consists of 943 objects in five fields selected without regard to color, morphology, or environment. Of these 943 objects, 730 are not stars or quasars (defining these spectroscopically rather than morphologically), and of these galaxies, redshifts have been secured for 591 (81%) with a median $\langle z \rangle = 0.56$. The reliability of these identifications has been confirmed by a large number of repeat observations (see CFRS III), and the nature of the remaining unidentified galaxies can be inferred in most cases, at least in a statistical sense, from their photometric properties and from analysis of the identifications of a subset of objects that were initially unidentified but for which repeated observations secured a redshift (see CFRS V and § 2.4).

The surface brightness selection effects in the original photometric sample are well understood and should be minimal for most types of galaxy (CFRS I). The identifications in the spectroscopic sample have been shown to be unbiased in surface brightness relative to the original photometric sample (CFRS IV).

An additional attractive feature of the CFRS sample is that the sample spans 5 mag, $17.5 < I_{AB} < 22.5$, in the same areas of sky, and the objects that were observed spectroscopically were selected from this range without regard to apparent magnitude (CFRS II). Thus, at any redshift, the bright and faint ends of the luminosity function are determined from exactly the same volumes of space.

2. CALCULATION OF THE LUMINOSITY FUNCTION

We have computed luminosity functions in the rest-frame B band from the statistically complete sample of 730 galaxies defined in CFRS II–CFRS V using a simple $1/V_{max}$ formalism (Felten 1976). The luminosity functions were calculated and cross-checked using two independently written codes (by S. J. L. and L. T.).

2.1. *The k-Corrections*

The $(V-I)_{AB}$ color straddles the rest-frame B band for $0.2 < z < 0.9$. Thus, for each galaxy, we first assign a spectral type by comparing the observed $(V-I)_{AB}$ colors, available for all objects, with those computed at that redshift from the spectral energy distributions given by CWW. As in Lilly (1993), an interpolation scheme is used whereby the CWW elliptical spectral energy distribution is assigned to spectral type 0, their Sbc to type 3, their Scd to type 5, and their Irr to type 6 with other spectral types representing interpolations between these. This spectral type (a real number) then defines the complete spectral energy distribution by interpolation from the CWW spectral energy distributions.

Since we wish to compute an absolute magnitude in the B band from I-band observations, we then compute a "k-correction color" for each galaxy from its assigned rest-frame spectral energy distribution. This k-correction color is computed from the interpolated spectral energy distribution as $(B-I_z)_{AB}$, where the subscript z indicates that the wave band is shifted to shorter wavelengths by a factor of $(1+z)$. The k-correction color is in effect a modeled interpolation of the observed $(V-I)_{AB}$ color for the redshift range $0.2 < z < 0.9$ and is the quantity plotted in Figure 1*b* for three spectral energy distributions.

The absolute magnitude in the rest-frame B band is then computed based on the isophotal I_{AB} magnitude, the distance modulus calculated from the luminosity distance, the bandwidth stretching term, and the k-correction color $(B-I_z)_{AB}$:

$$M_{AB}(B) = I_{AB} - 5 \log (D_L/10 \text{ pc}) + 2.5 \log (1+z) + (B-I_z)_{AB} .$$

It should be noted that the last two terms could be rewritten as a conventional k-correction for the I band plus a rest-frame $(B-I)_{AB}$ color derived from the spectral energy distribution. The luminosity distance is defined as

$$D_L = (c/H_0)(1+z)Z_q(z) ,$$

where $Z_q(z)$ is the function

$$Z_q(z) = \frac{\{q_0 z + (q_0 - 1)[(1+2q_0 z)^{0.5} - 1]\}}{q_0^2(1+z)} .$$

As noted above, since the $(V-I)_{AB}$ color straddles the rest-frame B for $0.2 < z < 0.9$, this procedure should lead to very small uncertainties in the computation of $M_{AB}(B)$ over this range, and none at all at $z \sim 0.2$ and at $z \sim 0.9$ (when the observed-V or observed-I corresponds to rest-B). For some purposes it has proved convenient to characterize the assigned rest-frame spectral energy distribution by the rest-frame $(U-V)_{AB}$ color. This roughly corresponds to the observed $(V-I)_{AB}$ at $z \sim 0.5$.

2.2. *Calculation of the Luminosity Function*

Since the form of the luminosity function at high redshift was unknown, the luminosity function was computed directly in bins of absolute magnitude, color, and redshift space using the $1/V_{max}$ formalism:

$$\phi(M, \text{color}, z)dM = \sum_k \frac{1}{V_{max}} .$$

The sum is carried out over all galaxies in the sample lying within the specified range of luminosity, color, and redshift. The V_{max} is computed as the comoving volume within which each galaxy (as defined by its absolute magnitude and assigned spectral energy distribution) would remain in the sample in

question, i.e., would satisfy the limits in apparent magnitude of the survey $17.5 < I_{AB} < 22.5$ and/or the limits in redshift of the bin. Writing the upper and lower limits of the redshift bin as z_U and z_L and the redshifts at which the object in question would have $I_{AB} = 17.5$ and $I_{AB} = 22.5$ as $z_{17.5}$ and $z_{22.5}$, respectively, then we have

$$V_{max} = \left(\frac{c}{H_0}\right)^3 d\Omega \int_{max\,(z_L,\, z_{17.5})}^{min\,(z_U,\, z_{22.5})} \frac{Z_q^2(z)}{(1+z)(1+2q_0 z)^{1/2}}\, dz\ .$$

The volume is based on an effective solid angle, $d\Omega$, of the survey of 112 arcmin^2 (CFRS II).

2.3. *Binning in Absolute Magnitude*

A magnitude-limited sample such as the CFRS has widely varying numbers of objects with different luminosities. In order to avoid having very small numbers of objects in some bins or unnecessarily losing luminosity resolution where there were many objects, we adopted a scheme whereby the size of the magnitude bin was allowed to vary so as to include roughly equal numbers of objects in each bin.

As noted above, the range of k-correction colors at a given redshift within the galaxy population (even if it is subdivided into color bins) means that, unless the observed wave band exactly matches the desired rest-frame wave band (so that the k-correction color is zero for all spectral types), the highest and lowest bins in absolute magnitude will be populated by only a subset of the galaxy population (i.e., the reddest or bluest objects within the population or color bin). In an I-band selected sample, this effect is modest and is zero at $z = 0.89$ if the luminosity function is calculated in the rest-frame B band. To avoid any such problems, we have simply eliminated the faintest few tenths of a magnitude in setting the bins for the luminosity functions at higher and lower redshifts. As shown in Figure 1*b* the range of k-correction increases roughly linearly as the redshift changes away from $z = 0.89$, so the amount of the luminosity function eliminated in this way was simply set to $0.6 \times |(z - 0.89)|$.

2.4. *Calculation of Uncertainties*

Uncertainties in the luminosity functions were calculated using a bootstrap algorithm in which the galaxy sample was resampled in a series of 1000 Monte Carlo simulations. In each simulation, a new sample of galaxies equal in number to the original sample was generated by randomly sampling the galaxies in the original sample (i.e., allowing both duplications and omissions of some of the original galaxies). This method takes into account the variable weighting of objects in the $1/V_{max}$ algorithm but does not take into account any effects of the clustering of galaxies in redshift space.

Assuming the clustering is independent of absolute magnitude, the small-scale clustering of galaxies in redshift space leads to an effective reduction in the number of independent galaxies, and this will lead to an increased uncertainty (by a factor of approximately $2.5^{1/2}$—see CFRS VIII) in the density normalization ϕ^* of any given redshift bin. In practical terms, the statistical uncertainty in ϕ^* arising from the numbers of objects, $N^{-0.5}$, is much smaller than the uncertainty that arises because of correlated uncertainties with the other parameters in any fitting of the luminosity function.

2.5. *Treatment of Unidentified Sources*

The CFRS complete sample of 943 sources contains 200 stars and six quasars (which were ignored for the present analysis), 591 confirmed galaxies with redshifts, and 146 unidentified objects. Seven of the unidentified objects are very likely to be stars based on their morphologies and colors (see CFRS V), and these were also eliminated from further consideration. The unknown nature of the remaining 139 galaxies represents a basic uncertainty in constructing the luminosity function. These objects are found toward the faint limit of the survey. The identification rate for galaxies (i.e., once the known stars and quasars are removed) as a function of I_{AB} magnitude is shown in Figure 7 of CFRS V.

The uncertainty introduced by the unidentified objects has been addressed in three different ways. We have first simply ignored the unidentified galaxies. This results in a "minimal" luminosity function that is based on only those galaxies that were actually identified. This is clearly the most conservative treatment, but it results in a luminosity function that must at some level be an underestimate of the true luminosity function. Second, we have followed the usual procedure of weighting the galaxies with known redshifts by the inverse of the fractional identification rate of the sample (calculated after the stars and quasars were removed), determining this as a function of magnitude. In essence, this scheme incorporates them into the sample, making the implicit assumption that they have the same color and redshift distribution as the identified galaxies in the sample at the same magnitude. We refer to this as the "weighted" luminosity function.

This weighting scheme seems unnecessarily restrictive because, as discussed in detail in CFRS V, we have a good idea of what the unidentified objects are from two separate lines of argument. First, in the course of the project, 99 unidentified objects were reobserved and identifications subsequently secured for approximately 70% of these objects (see CFRS III). If we make the assumption that these 99 reobserved objects are similar to the roughly 110 objects that were unidentified and that were not reobserved, then we can say that the redshift distribution of about half of the final list of 139 unidentified objects is known, at least statistically, and is given by the redshift distribution of the "recovered failures." Second, as described in CFRS V, we devised a simple redshift estimator based on an empirical comparison of the $(V-I)_{AB}$ and $(I-K)_{AB}$ colors, the I_{AB} magnitude, and the compactness of the images, with a learning sample given by galaxies with secure redshifts. This estimator successfully reproduced the redshift distribution of the "recovered failures." It was then applied to all 139 unidentified objects in the final catalog, with the one minor, and ad hoc, alteration that 20 galaxies were arbitrarily placed at $z > 1$, where our observational set-up created a strong bias against absorption line objects (see CFRS V for a detailed discussion). Our third approach to calculating the luminosity function was thus based on placing the unidentified objects at their estimated redshifts. This obviously means that we cannot consider the luminosity function for these red galaxies at $z > 1$. We refer to this third estimate as the "best estimate" luminosity function.

2.6. *Representation of the Luminosity Function*

As with other flux density–limited samples, most of the galaxies in the CFRS occupy a small range of apparent magnitude, and thus the typical absolute magnitudes in the sample are correlated with distance. At very low redshifts, this effect is dealt with when constructing local luminosity functions through a straightforward volume correction, and the resulting luminosity function is defined over a wide range of lumi-

nosities. In the case of a deep sample such as the CFRS, the range of distances sampled corresponds to a wide range of cosmic epochs, and thus, at each epoch, only a limited range of luminosities is present in the sample. A simple volume correction is inappropriate if evolution in the population is a possibility.

Consequently, only a relatively short segment of the luminosity function can be determined at each epoch from the CFRS. This makes it dangerous to fit the usual Schechter function—the individual parameters will be poorly determined, and the uncertainties in the parameters are inevitably highly coupled. Furthermore, the parameters of the Schechter function (such as the "faint end slope," α, or the "knee," M^*) that result when the function is fitted over a small range of luminosities (as would be the case here) respond to features that may be quite unconnected with their intuitive meanings, and thus the changes of the parameters with redshift could be quite misleading.

The philosophy adopted in the present work is to compare the luminosity functions at different epochs as nonparametrically as possible (i.e., directly point-by-point) rather than to fit analytic functions and interpret changes in the parameters of these fits. However, as an aid in translating our results from diagram to diagram and to enable other workers to reproduce our luminosity function on their own diagrams, we have fitted analytic functions to our luminosity functions. We could have chosen any functional representation, such as a polynomial, but we chose to use the Schechter function. The fits were simple χ^2 minimizations on the binned luminosity function, with the model being integrated across each luminosity bin.

The parameters of these various fits (without formal uncertainties) are listed in Table 1, along with the range of $M_{AB}(B)$ over which they are valid. *We stress that these are representations of our data over a limited luminosity range and are not intended to be "determinations" of the Schechter parameters.* The changes in individual parameters, such as α, M^*, and ϕ^*, should not be viewed in isolation.

3. THE POPULATION OF GALAXIES $0.0 < z < 1.3$

3.1. *The Trivariate Luminosity Function*

The CFRS sample is sufficiently large that we can subdivide the sample into several redshift bins and into two color bins

TABLE 1

PARAMETERS OF SCHECHTER FUNCTION SEGMENTS

Type[a]	q_0	Color Sample[b]	z (Range)	$-M_{AB}(B)$(Range)	α	$M^*_{AB}(B)$	ϕ^*
Minimal.....	0.5	All	0.00–1.30	16.0–23.0	0.89	−21.19	0.0041
			0.20–0.50	17.2–22.8	0.85	−20.81	0.00378
			0.50–0.75	19.7–22.9	0.35	−20.84	0.00552
			0.75–1.00	20.0–23.0	0.67	−21.06	0.00499
		Red	0.20–0.50	17.5–22.3	0.00	−20.41	0.0035
			0.50–0.75	19.5–22.5	0.00	−20.80	0.0023
			0.75–1.00	20.0–23.0	1.40	−23.00	0.00026
		Blue	0.20–0.50	18.0–21.5	1.61	−22.15	0.00030
			0.50–0.75	19.3–23.0	0.86	−21.15	0.0029
			0.75–1.00	20.2–22.5	1.09	−21.16	0.0041
			1.00–1.30	21.0–23.5	2.50	−22.87	0.00012
Best.....	0.5	All	0.20–0.50	17.2–22.8	1.03	−21.04	0.0034
			0.50–0.75	19.7–22.9	0.50	−20.83	0.0078
			0.75–1.00	20.2–23.0	1.28	−21.24	0.0068
		Red	0.20–0.50	17.5–22.3	0.00	−20.44	0.0037
			0.50–0.75	19.5–22.5	0.37	−21.00	0.0026
			0.75–1.00	20.0–23.0	2.01	−23.00	0.00018
		Blue	0.20–0.50	18.0–21.5	1.34	−20.83	0.0013
			0.50–0.75	19.3–23.0	1.07	−21.32	0.0030
			0.75–1.00	20.2–22.5	1.56	−21.40	0.0038
			1.00–1.30	21.0–23.5	2.50	−22.87	0.00012
	0.0	All	0.20–0.50	17.5–22.5	1.10	−21.37	0.00193
			0.50–0.75	19.5–23.5	0.60	−21.28	0.00375
			0.75–1.00	21.0–23.5	1.68	−22.16	0.00150
		Red	0.20–0.50	17.5–22.5	0.22	−20.86	0.0024
			0.50–0.75	19.5–22.7	0.00	−21.04	0.0017
			0.75–1.00	20.5–23.5	1.87	−22.99	0.00018
		Blue	0.20–0.50	18.0–21.5	1.49	−21.40	0.00063
			0.50–0.75	19.5–23.5	1.09	−21.66	0.0018
			0.75–1.00	20.8–22.8	1.86	−22.21	0.0010
			1.00–1.30	21.5–23.5	2.50	−22.99	0.00012

NOTE.—Because of the small range of absolute magnitudes available at each redshift and the highly coupled nature of the three parameters in the Schechter function when fitted over a small range, the parameters in the last three columns of the table should not be taken in isolation but rather should, together, be viewed as defining the luminosity function in the absolute magnitude range given in the fifth column.

[a] This refers to the treatment of the unidentified objects. In the "minimal" treatment they are ignored, and in the "best" treatment they are assigned estimated redshifts as described in the text. The latter is regraded as the best estimate of the actual luminosity function.

[b] Red and Blue refer to samples divided by the rest-frame color of an unevolving Sbc galaxy, taken to be $(U-V)_{AB} = 1.38$.

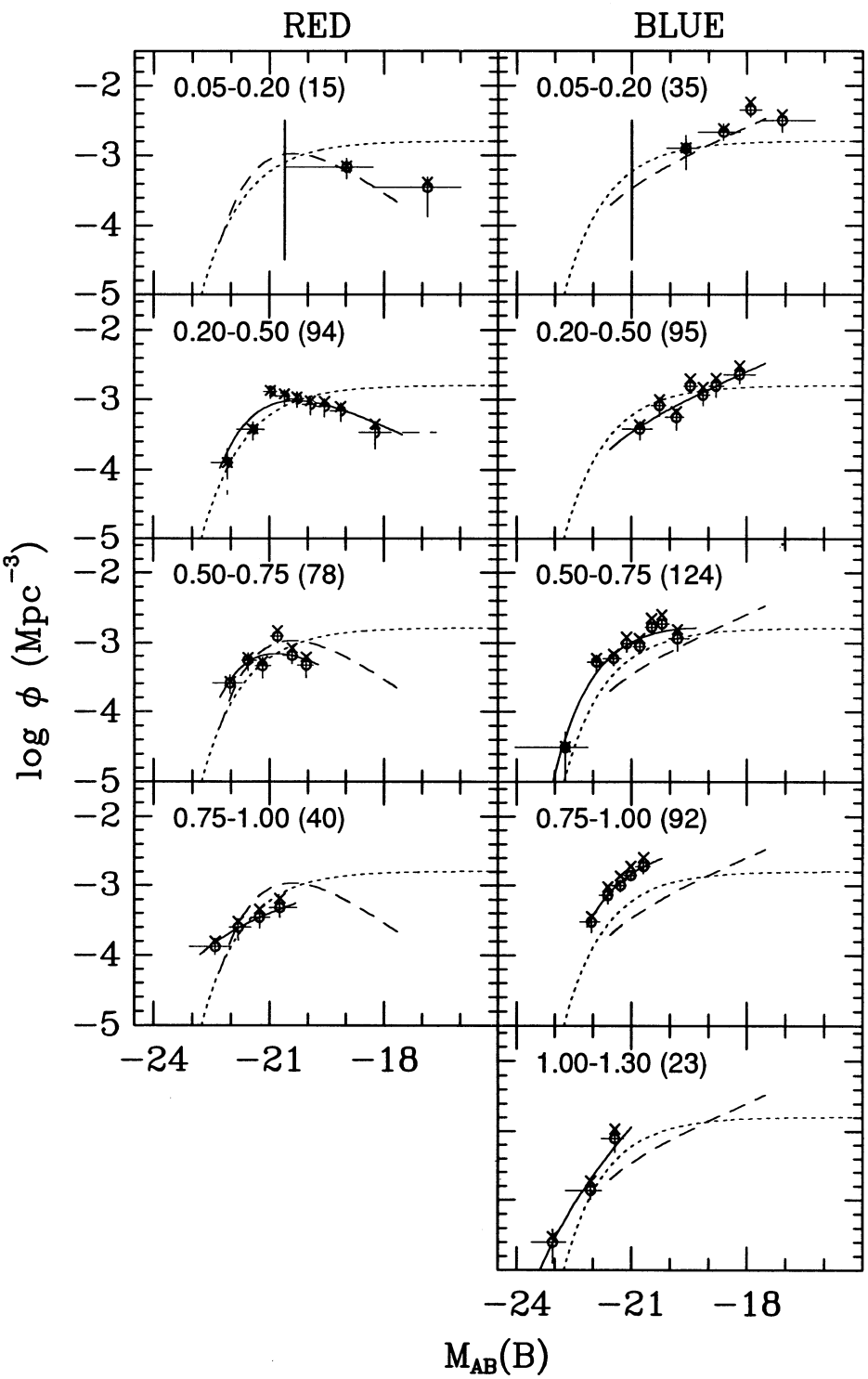

FIG. 2a

FIG. 2.—(*a*) The "minimal" and "weighted" luminosity functions (see text) for the CFRS sample split by redshift (vertically as indicated by the label in each panel) and intrinsic color (redder than CWW Sbc on the left, bluer on the right). Redshift range and number of objects in that range are indicated by the label in the upper left of each panel. The vertical bar in the $0.05 < z < 0.2$ bin indicates luminosities excluded by the bright end magnitude limit of the survey. Each panel at $z > 0.2$ shows a Schechter function fitted to the "minimal" luminosity function (*solid curve*), the fit for the luminosity function at $0.2 < z < 0.5$ (*dashed curve*), and the Loveday et al. (1992) overall luminosity function, which is not split by color (*dotted curve*). (*b*) As in (*a*) except that the "best estimate" luminosity function (see text) is shown. (*c*) As in (*a*) and (*b*) except that the "best estimate" luminosity function is calculated assuming $q_0 = 0.0$.

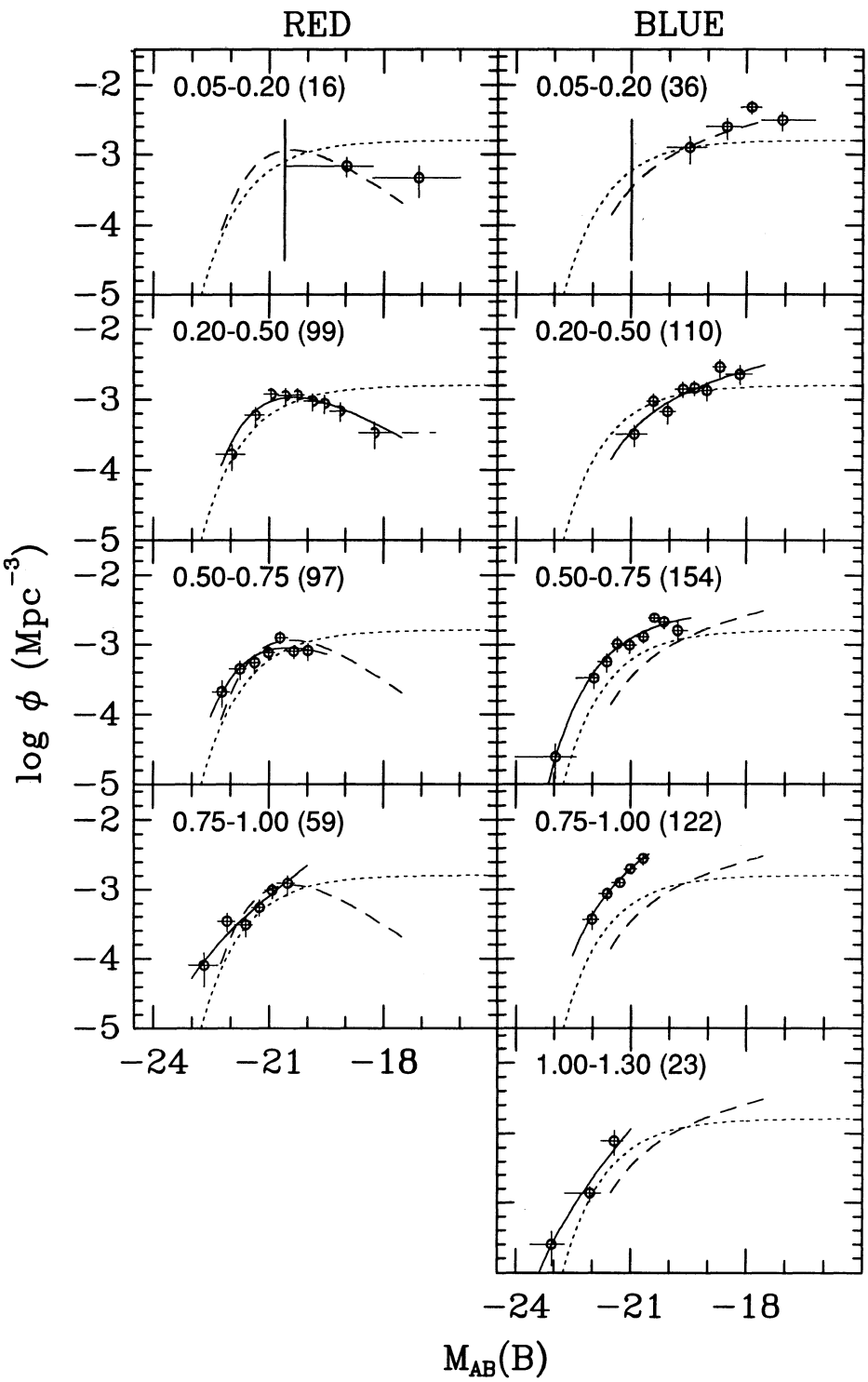

FIG. 2*b*

and still have reasonable numbers of objects with which to construct the trivariate luminosity function $\phi(M, \text{color}, z)$.

We show in Figures 2*a*–2*c* four computations of the luminosity function in which the sample has been split into blue and red populations (by rest-frame color—dividing the sample at the spectral energy distribution of the CWW Sbc galaxy, roughly the median spectral type) and into five redshift intervals: $0.05 < z < 0.2$, $0.2 < z < 0.5$, $0.5 < z < 0.75$, $0.75 < z < 1.0$, and $1.0 < z < 1.3$ (blue galaxies only). The choice of these redshift bins is to some degree arbitrary but was motivated as follows: In an $\Omega = 1$ cosmology, the first two bins correspond to intervals in cosmic time of $0.2\tau_0$ centered on $0.85\tau_0$ and $0.65\tau_0$, respectively. The next two redshift bins correspond to intervals of about $0.1\tau_0$ centered on approximately

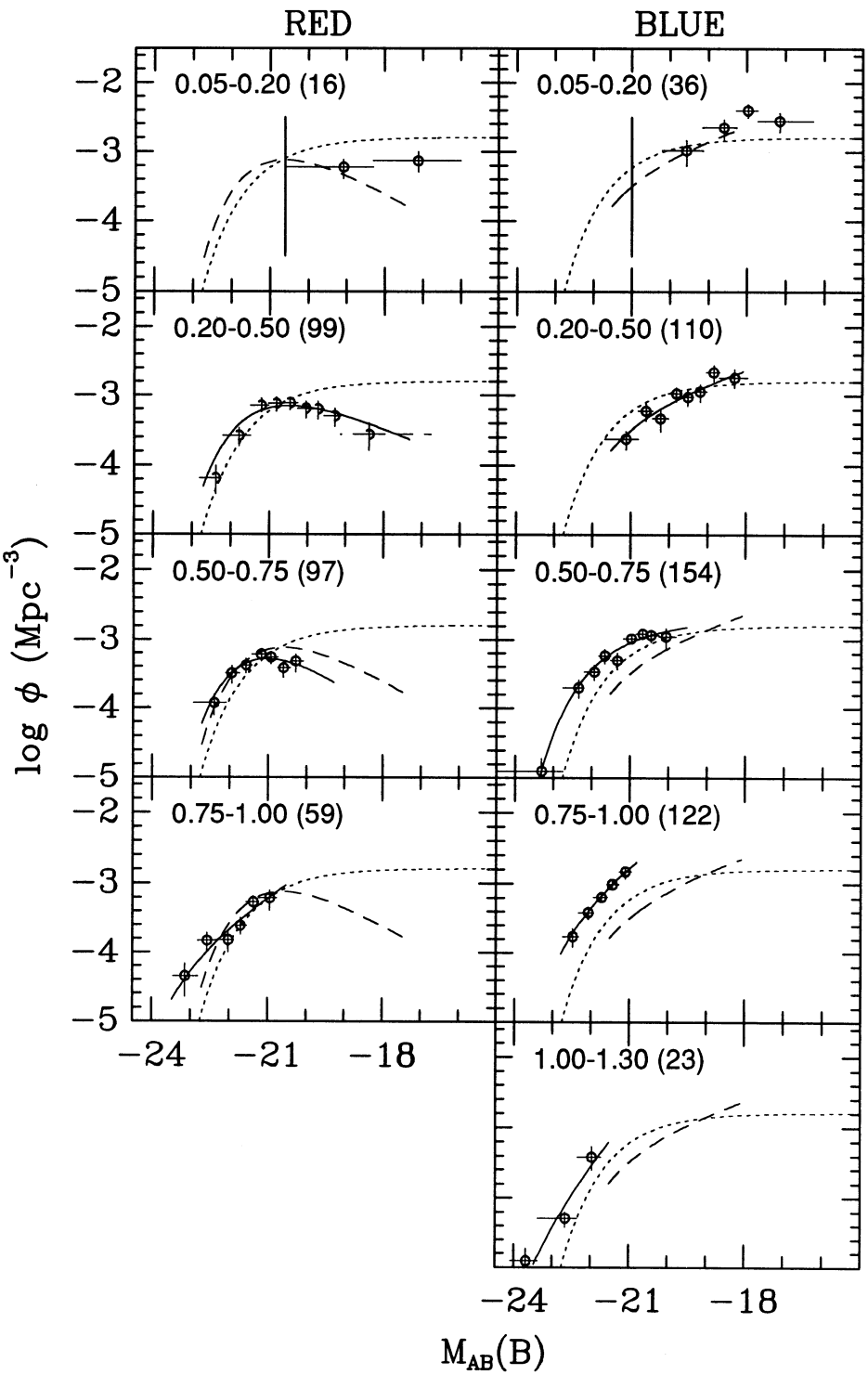

FIG. 2c

$0.5\tau_0$ and $0.4\tau_0$. It should be noted that the upper magnitude limit of $I_{AB} > 17.5$ excludes galaxies with $M_{AB}(B)$ brighter than between -20.5 and -21.0 (depending on their color) from the lowest redshift $0.05 < z < 0.2$ bin. The excluded region of the luminosity function is to the left of the vertical lines in the top two panels of Figures 2*a*–2*c*. Figure 2*a* shows both the "minimal" luminosity function and the "weighted" luminosity function for $q_0 = 0.5$, Figure 2*b* shows the "best estimate" luminosity function for $q_0 = 0.5$, and Figure 2*c* shows the "best estimate" luminosity function for $q_0 = 0$.

In each of the panels at $z > 0.2$ in Figure 2, we plot the segment of the Schechter function that has been fitted to the luminosity function in that redshift range as a solid curve. We also show in each panel the fits to the $0.2 < z < 0.5$ blue and

red luminosity functions (*dashed curves*) along with the Loveday et al. (1992) local luminosity function (*dotted curve*). It should be noted that this latter is derived from the whole galaxy population of Loveday et al., not split by morphological or spectral type, and is provided primarily as a reference point within the diagram. With the important caveats discussed in § 2.6 (i.e., that these are *representations* of the data, not *determinations* of the parameters), the parameters of the Schechter segments are given in Table 1.

Comparison of Figures 2*a*–2*c* shows that the qualitative features of the luminosity function are largely independent of the treatment of the unidentified objects (and, to a certain degree, of the value of the deceleration parameter q_0). In detail, it can be seen that the "best estimate" luminosity function is slightly steeper than the "minimal" one since the unidentified objects are concentrated at the faint end of the sample and thus at the faint end of the luminosity function at any redshift. An additional small effect is that the increase relative to the "minimal" luminosity function is larger at $z > 0.5$, which reflects the fact that the distribution of estimated redshifts is shifted slightly to higher redshifts than that of the sample as a whole (CFRS V).

In what follows we concentrate on Figure 2*b*, which represents our best estimate of the luminosity function for $q_0 = 0.5$, before seeing how the situation would change if $q_0 \sim 0$. There are three interesting results apparent in Figure 2*b*, which we describe phenomenologically in the next three subsections. We then present two further analyses that illustrate these effects in §§ 3.2 and 3.3 before discussing, in § 3.4, the possible origin and cosmological context of these results.

3.1.1. *The Local Luminosity Function: Is There Evolution at* $0.0 < z < 0.2$?

The CFRS was designed to produce a homogeneous sample of galaxies at $z > 0.2$, and there are only 50 galaxies at $z < 0.2$. However, there is clear evidence in Figure 2 for a population of faint galaxies [$M_{AB}(B) \sim -18$] in the lowest redshift bin $0.05 < z < 0.2$ (which we might expect to be a "local" population) that has a significantly higher comoving number density than in the local luminosity function of Loveday et al. (1992), an effect also noticed in their smaller sample by Tresse et al. (1993). Comparison of the upper two levels on Figures 2*a*–2*c* shows that this low-redshift, low-luminosity population is well matched by our luminosity functions at $0.2 < z < 0.5$. Indeed, *within our sample* we see no evidence per se for evolutionary changes in the galaxy population between the $0.05 < z < 0.2$ and $0.2 < z < 0.5$ redshift bins, although there are significant differences with the Loveday et al. (1992) local luminosity function.

As noted above, our luminosity function at $z < 0.2$ contains no luminous galaxies with $M_{AB}(B) < -20.5$ because of the bright end limit of our sample ($I_{AB} > 17.5$), and so we cannot state categorically whether the differences with Loveday et al. (1992) represent a difference in the overall normalization of the luminosity function (i.e., a different ϕ^*) or a difference only at the faint end, although we strongly suspect the latter. At higher redshifts, $0.2 < z < 0.5$, our Schechter function fits for the "best estimate" luminosity function [over the approximate luminosity range $-22.5 < M_{AB}(B) < -17.5$] are $\alpha = 1.03 \pm 0.15$, $M^*_{AB}(B) = -21.04 \pm 0.25$, $\phi^* = 0.0031 \pm 0.00095$ Mpc^{-3}. These are similar to the values of Loveday et al. (1992) except for an elevated ϕ^* by a factor of 1.8.

This excess at faint magnitudes is similar in size, though a little higher in luminosity, to that which appears in the luminosity function derived from the CfA sample by Marzke et al. (1994a). The excess evident in their Figure 9*b* at $M \sim -15.75$ would appear in our figure at $M_{AB}(B) \sim -17.5$ once allowance is made for the different values of H_0 used and the zero-point offset between B and B_{AB}. In both samples an excess of approximately a factor of 4 over the luminosity function of Loveday et al. (1992) is observed.

There are very few published local luminosity functions that are split by color. The most directly comparable is that quoted by Metcalfe et al. (1991). We show in Figure 3 our $0.05 < z < 0.2$ and $0.2 < z < 0.5$ luminosity functions, split as in Figure 2 by the implied rest-frame $(U-V)$ color [though at these low redshifts our $(V-I)$ observed color more closely

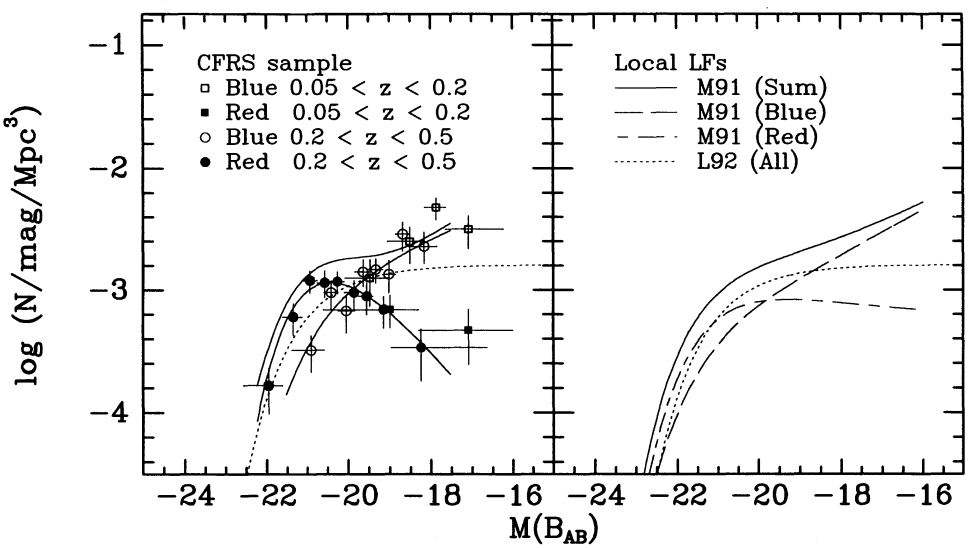

FIG. 3.—*Left*: the CFRS "best estimate" luminosity function split by color for $0.05 < z < 0.2$ and $0.2 < z < 0.5$. Solid lines are Schechter function segments fitted to the blue and red data separately, and the sum of these. The dotted curve is the Loveday et al. (1992) luminosity function, which is not split by color. *Right*: The color-dependent luminosity function from Metcalfe et al. (1991) split at $(B-V) = 0.72$, again compared with the Loveday et al. (1992) luminosity function. There is good agreement between the two color-dependent luminosity functions, which both show an excess over the Loveday et al. (1992) faint end (see also Marzke et al. 1994a)

matches the rest-frame $(B-R)$] and the local luminosity function, split at $(B-V) = 0.72$, derived by Metcalfe et al. (1991). These are extremely similar. The steep slope of the luminosity function of bluer galaxies ($\alpha = 1.30 \pm 0.25$) is also seen indirectly in Marzke et al.'s (1994b) decomposition of the CfA luminosity function into different morphological bins.

A fair conclusion at this point is that uncertainties in the local luminosity function are sufficiently large as to make the determination of whether there is evolution back to $z \sim 0.2$ (cf. Broadhurst et al. 1988) rather hard. At higher redshifts, we have the advantage that the luminosity function can be constructed from our single CFRS sample, removing many of these ambiguities, and so evolutionary changes are much more secure.

3.1.2. *No Change in the Luminosity Function of Redder Galaxies* $0.2 < z < 1.0$

The luminosity function of the redder galaxies (redder than the present-day CWW Sbc spectral energy distribution) represented in the panels on the left of Figure 2*b* clearly shows remarkably little change with epoch back to the highest redshifts encountered, $z \sim 1$. The fit to the $0.2 < z < 0.5$ luminosity function is clearly a reasonable representation of the luminosity function of red galaxies at $0.5 < z < 0.75$ and $0.75 < z < 1.0$ and, as noted above, within the accessible range of luminosities, also at $0.05 < z < 0.2$. This presumably implies that the population of ellipticals and bulge-dominated spirals is roughly constant with epoch. While one can imagine combinations of evolutionary processes that could produce the appearance of a static population as in Figure 2*b*, there is little evidence per se either for a substantial decrease with increasing redshift in the numbers of these redder galaxies, as might be expected if the population had been formed recently through the merger of massive actively star-forming subunits, or for a brightening of more than a few tenths of magnitude from the passive evolution of the dominant old stellar populations in these galaxies (cf. Tinsley & Gunn 1976; Bruzual 1983; Yoshii & Takehara 1988; Bruzual & Charlot 1993). We return to this below.

In order to try to quantify this lack of change in the luminosity function of the redder galaxies, a Schechter function was first fitted to the luminosity function of these galaxies over the whole range $0 < z < 1$. This yielded $\alpha = -0.5$, $M^*_{AB}(B) = -21.00$, and $\phi^* = 0.00185$ Mpc^{-3}. Keeping α fixed at this value, but allowing M^* and ϕ^* to vary, Schechter functions were then fitted to the red luminosity functions in the three redshift bins $0.2 < z < 0.5$, $0.5 < z < 0.75$, and $0.75 < z < 1.0$. The 1 σ error ellipses for the two free parameters in these fits are shown in Figure 4. It should be noted that the fit for $z > 0.75$ is least well constrained because nearly all the galaxies have $M^*_{AB}(B) < -21.0$ at these redshifts.

Clearly, these fits are consistent with no change at all in either M^* or ϕ^* over the whole redshift range. However, they are also consistent with a modest brightening with look-back time if accompanied by a decrease in the total number of objects. Over the interval from $z \sim 0.3$ to $z \sim 0.6$, a brightening of at most 0.5 mag and a decrease of at most 33% in the comoving space density of these red galaxies would be acceptable.

3.1.3. *Evolution in the Luminosity Function of Bluer Galaxies* $0.2 < z < 1.0$

In contrast to the luminosity function of red galaxies, the luminosity function of the bluer galaxies (i.e., bluer than the present-day CWW Sbc) shown in the right-hand panels of Figure 2*b* shows significant changes as the redshift increases. In general terms, this may be characterized by a brightening of the luminosity with look-back time, although the same effect could, of course, also be produced by an increase in comoving density. In terms of luminosity evolution, this appears to be differential with luminosity and to "saturate" at the bright end, producing a steepening of the luminosity function. Between $0.2 < z < 0.5$ and $0.5 < z < 0.75$, the luminosity function in Figure 2*b* brightens by about 1 mag, while in the next step to $0.75 < z < 1.0$ there is no change in the bright end but a further brightening of about 1 mag around $M_{AB}(B) \sim -20$. The saturation at bright magnitudes is evident also in the final $1.0 < z < 1.3$ bin, which shows little change relative to the $0.75 < z < 1.0$ bin for $M_{AB}(B) < -21.5$.

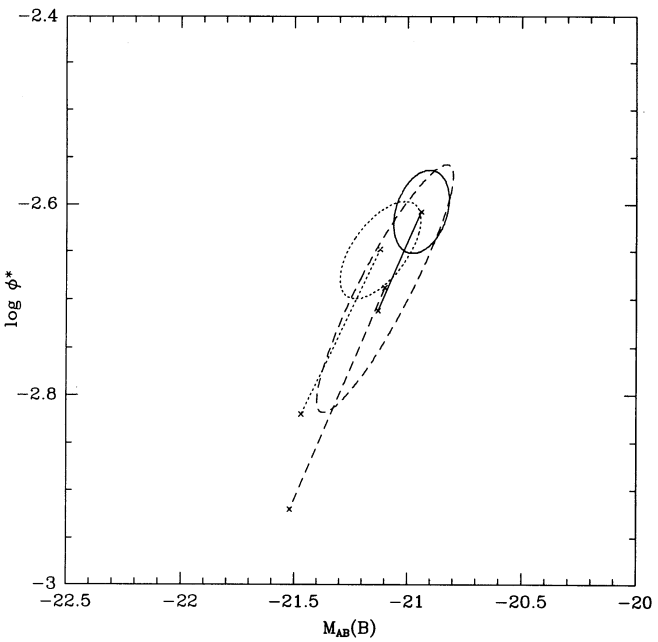

FIG. 4.—Error ellipses for $M^*_{AB}(B)$ and ϕ^* obtained by fitting a Schechter function with $\alpha = -0.5$ to the $q_0 = 0.5$ luminosity functions of red galaxies (Fig. 3*b*, *left-hand panels*) in the three redshift intervals $0.2 < z < 0.5$ (*solid curve*), $0.5 < z < 0.75$ (*dotted curve*), and $0.75 < z < 1.0$ (*dashed curve*). These show that the luminosity functions are consistent with either no change in either parameter or with a combination of modest brightening and decreasing comoving density with increasing redshift. The vectors emanating from each ellipse show the effect of changing q_0 to $q_0 = 0$.

Because our redshift baseline is so large, the evolution of the galaxy luminosity function is evident within our single sample and is thus independent of any uncertainties in the definition of the "local" population. We regard Figure 2 as providing incontrovertible evidence that the galaxy population changes with cosmic epoch and believe that the "no-evolution" scenario advocated by Koo et al. (1993) is thus no longer tenable.

3.1.4. *Results with* $q_0 = 0$

The effect of changing q_0 to lower values is straightforward. There is little change at the lower redshifts, and at higher redshifts, the different populations have lower comoving densities but higher luminosities, i.e., they tend to move diagonally down and to the left in the diagrams.

For the red galaxies, this increases the amount of passive luminosity evolution that is permitted since the high-redshift population will be intrinsically more luminous. It also allows a larger increase in the comoving density since $z \sim 1$, because the

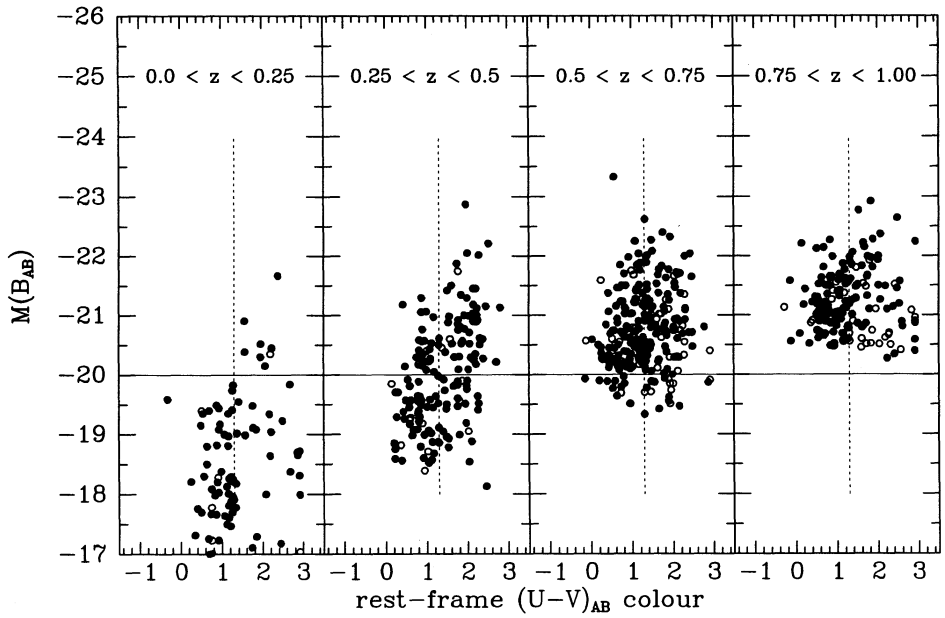

FIG. 5.—Rest-frame color-magnitude diagrams for the CFRS sample. Objects with open symbols have estimated redshifts (see text). At constant luminosity (e.g., above the horizontal line), the increase in luminosity of the blue galaxies relative to the red galaxies at $z > 0.5$ is apparent.

comoving density of the red population will be lower for $q_0 \sim 0$ at the earlier epochs. We have represented these changes as vectors emanating from the centers of the error ellipses in Figure 4.

For the blue galaxies, the effect of moving the luminosity functions down and to the left has little effect on the amount of evolution required. There is still a requirement for the equivalent of approximately 1 mag of luminosity evolution to $z \sim 0.6$ and for additional evolution to $z \sim 0.9$ at $M_{AB}(B) \sim -21$.

3.2. *The Rest-Frame Color-Magnitude Diagrams at Different Epochs*

In Figure 5, color-magnitude diagrams are plotted for galaxies in the sample in different bins of redshift. The absolute B magnitude calculated as above is plotted against the rest-frame $(U-V)_{AB}$ color computed for the interpolated spectral energy distribution that matches the observed $(V-I)_{AB}$ color. As noted above, these colors are exactly equivalent at $z \sim 0.5$, and the transformation at other redshifts is modest. The unidentified galaxies with estimated redshifts (see above and CFRS V) are shown as open symbols.

In a magnitude-limited sample such as the CFRS, the mean absolute magnitude increases with redshift because of the bright and faint sample limits and the obvious volume effects. If attention is confined to objects brighter than $M_{AB}(B) = -20$ (1 mag below present-day L^*), then the increase with redshift of the luminosity of the blue population of galaxies, relative to the red population, seen on Figure 3, is clearly apparent in Figure 5. The well-defined color-luminosity relation present at low redshifts is eliminated at the higher redshifts by the emergence of the population of bright blue galaxies.

3.3. *V/V_{max} as a Function of Spectral Type*

As has been known for many years (Schmidt 1968), the statistics of the locations of objects within their observable volumes V_{max}, computed as above, gives information on the evolution of that population. Values of 0.5 indicate a homogeneous unevolving population, while values greater than 0.5 indicate a population whose comoving density, at a given luminosity, is increasing with distance. In order to see which spectral types are producing the evolution seen in Figures 2 and 5, the V/V_{max} statistic has been computed for galaxies in the redshift range $0.3 < z < 1.0$ as a function of spectral type, with the results shown in Table 2 for $q_0 = 0.5$ (the V/V_{max} statistic is insensitive to q_0). This redshift range was chosen since it is the range over which the spectral typing of galaxies from their $(V-I)_{AB}$ colors is most accurate and over which there should be little bias in the determination of redshifts as a function of spectral type (see CFRS IV and CFRS V for a discussion).

The values of V/V_{max} show a clear increase toward bluer galaxy spectral types, increasing from about 0.5 for galaxies redder than our spectral type 3 (i.e., the Sbc galaxy of CWW) to greater than 0.6 for the bluest galaxies. This is consistent with the changes seen in the luminosity function (Fig. 2*b*) and color-magnitude diagrams (Fig. 5).

3.4. *Discussion: The Evolving Galaxy Population*

The above analyses show that the galaxy population in the $0.2 < z < 1$ interval is characterized by strongly differential evolution. The luminosity function of red galaxies changes little if at all, while the luminosity function of blue galaxies

TABLE 2

VALUES OF V/V_{max} FOR $0.3 < z < 1.0$

SED[a]	Spectral Class	$(U-V)_0$	N[b]	V/V_{max}
Elliptical.....	0	2.29	58	0.50 ± 0.04
	1	1.96	53	0.42 ± 0.04
	2	1.67	58	0.50 ± 0.04
Sbc.....	3	1.38	50	0.54 ± 0.04
	4	1.27	38	0.56 ± 0.05
Scd.....	5	1.15	95	0.56 ± 0.03
Irr.....	6	0.64	158	0.62 ± 0.02

[a] Spectral energy distribution from CWW that defines the spectral class used in this paper. Others are interpolated.

[b] Number of galaxies.

brightens considerably, coming up from low luminosities to eventually dominate the luminosity function around present-day L^*. Furthermore, within the blue population, there is evidence that the evolution is differential in luminosity, which leads to a steepening of the luminosity function. This picture broadly matches the heuristic model for the evolving galaxy population constructed by Lilly (1993) to match the observed counts in B, I, and K and the then available $N(z)$ distributions in B and I.

The significance of the unevolving red population is that in general terms, it supports the idea that massive, quiescent galaxies have been around in the universe for a considerable time and got most of their activity over with at early epochs, beyond the reach of present surveys. This is consistent with what is known about early-type galaxies in clusters to $z \sim 1$ (see, e.g., Dressler, Gunn, & Schneider 1985; Rakos & Schombert 1995).

The detailed interpretation of the lack of change in L^* of the red population requires knowledge of the strength of the so-called passive evolution that arises, even in populations formed in a single burst of stars, because of the changing number of turn-off stars and red giants. The strength of the passive evolution is strongly dependent on the slope of the initial mass function (Tinsley & Gunn 1976), and the behavior will be different for systems that continue to form stars. For instance, in the models of Yoshii & Takahara (1988) and Bruzual & Charlot (1993), while single-burst models fade by approximately 0.3 mag at a wavelength of 2 μm as they double in age, models with a constant star formation rate increase in brightness by the same amount. Thus, the luminosity evolution of composite stellar populations may be quite mild, and, for example, stellar populations with an exponentially declining star formation rate with e-folding time of order 7 Gyr have almost no luminosity change at 2.2 μm. Given the sensitivity to the poorly constrained initial mass function, we regard the amount of passive evolution as a quantity to be determined observationally, say from observations of the fundamental plane in clusters of galaxies at high redshift, if at all possible.

The nature of the evolving blue population is more intriguing. Although it would be straightforward to view this as arising from the brightening of individual objects by modest amounts (1–2 mag), it should be stressed that the luminosity function tells us only about the evolution of the population (defined in some observable way) and not about the evolution of individual objects or about the movement of objects into or out of the population in question. Our analysis cannot distinguish in a rigorous way between luminosity evolution and density evolution.

However, in the context of this ambiguity, the "excess" of low-luminosity galaxies above the flat ($\alpha \sim 1$) faint end of the Loveday et al. (1992) luminosity function, seen here and in the CfA luminosity function of Marzke et al. (1994a), is highly significant. These galaxies are attractive descendants for the bright blue galaxies seen with high number density in our luminosity function at high redshift, $z > 0.5$. It is important to appreciate that many of the more exotic interpretations that were advanced to account for the large numbers of blue galaxies seen even at quite bright magnitudes ($B < 24$) (such as bursting minihalos; Babul & Rees 1992, or wholesale merging of major mass concentrations; Broadhurst et al. 1992) were introduced to a large degree because of the difficulty of identifying a local population of sufficient number density if the local population was described by an $\alpha \sim 1$ flat luminosity function with low ϕ^*. Thus, it is noteworthy on Figure 2*b* that, within our whole sample, the highest comoving number density (per magnitude) is encountered in the lowest redshift $0.05 < z < 0.20$ bin at $M_{AB}(B) \sim -18$. Although these low-redshift, low-luminosity galaxies do not themselves contribute significantly to the total count at our magnitude level, they do represent a ready source population for the evolving brighter galaxies seen at $z > 0.5$ (with $-21 < M_{AB}(B) < -20$) that do dominate the sample.

Establishing whether the evolution in the population seen in Figures 2*b* and 5 is indeed due to a simple brightening with look-back time of the individual objects that are seen today as a population of moderate luminosity objects [$M_{AB}(B) \sim -18$] will require detailed examination of their properties and particularly of their morphologies and internal kinematics. Our investigations along these lines will be presented in due course elsewhere (e.g., Schade et al. 1995, hereafter CFRS IX). At this point, we simply note that the relatively normal morphologies, spectra, and colors of the blue galaxies at $z > 0.5$ do not at first sight support many of the more exotic models in which they represent a population that has disappeared by the present epoch. We also note that the clustering properties of these galaxies are consistent with those of local populations of star-forming galaxies if there has been plausible growth of large-scale structure in the universe (Le Fèvre et al. 1996, hereafter CFRS VIII; Hudon & Lilly 1996).

One final comment can be made about the practicality of the volumetric test for q_0 discussed by Loh & Spillar (1986). The CFRS sample is very similar in size and depth to the sample used by Loh & Spillar in which essentially all of the redshifts were estimated photometrically by comparing colors with model spectral energy distributions. The demonstration of strongly differential evolution of the luminosity function in color (and probably also in luminosity) in the present work will make any future application of this particular cosmological test difficult unless individual masses can be determined for a large number of galaxies. If it is assumed that the red galaxies form a stable population of fixed comoving number density (we believe that such an assumption would be quite unwarranted at the present time), then the values of ϕ^* derived in § 3.1.1 for the red galaxies alone clearly favor a value of q_0 larger than 0 (see Fig. 4). Making this assumption, it is found that $q_0 < 0.1$ is formally excluded with 90% confidence. We ascribe little weight to this result.

4. COMPARISONS WITH OTHER SAMPLES

The CFRS is considerably larger than any other current sample of faint galaxies, and this has allowed us to define the luminosity function to greater redshifts and with considerably finer sampling in color and redshift space than other studies. We review here the recent results of others based on smaller samples selected in different ways and argue that a broadly consistent picture emerges.

To facilitate comparisons with these other samples, the upper panel in Figure 6 shows the overall "minimal" and "weighted" luminosity functions constructed from the entire CFRS sample integrated over all $0.0 < z < 1.3$ and undifferentiated by color. A Schechter function fitted to the minimal luminosity function in the upper panel of Figure 6 gives $\alpha = -0.9 \pm 0.1$ and $M^*_{AB}(B) = -21.2 \pm 0.15$. These are remarkably close to the values found by Loveday et al. (1992) from the DARS local redshift survey ($\alpha = -0.97$ and $M_{AB}(B) = -21.0$, respectively); however, our value of ϕ^* (0.0041 ± 0.0004 Mpc^{-3}) is about 2.3 times as high as the

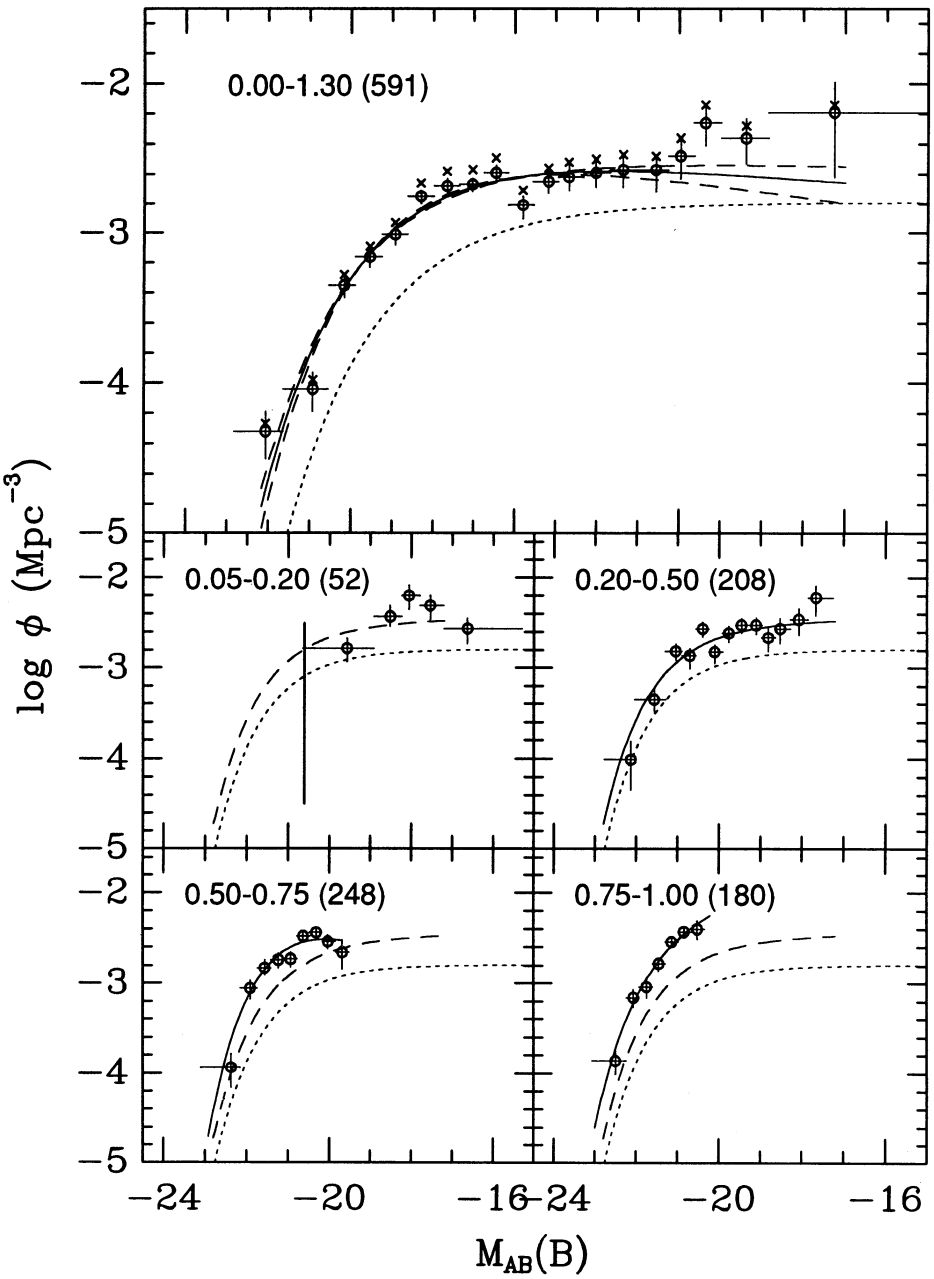

FIG. 6.—The upper panel shows the overall luminosity function for all CFRS galaxies in the $0.05 < z < 1.0$ redshift range. Circles with error bars are the "minimal" luminosity function, and the crosses represent the "weighted" luminosity function (see text). The solid and dashed curves represent fitted Schechter functions (best-fit and 1 σ fits), and the dotted curve represents the Schechter function found for local galaxies by Loveday et al. (1992). The four lower panels show the "best estimate" luminosity function (see text) split into four redshift bins. Redshift range and number of objects in that range are indicated by the label in the upper left of each panel. Galaxies to the left of the vertical line in the $0.05 < z < 0.2$ bin were excluded by the bright end magnitude limit of the survey. In each panel at $z > 0.2$, a Schechter function fitted to the luminosity function is shown (*solid curve*) along with the fit for the luminosity function at $0.2 < z < 0.5$ (*dashed curve*) and the Loveday et al. (1992) overall luminosity function (*dotted curve*).

Loveday value. The Loveday et al. (1992) Schechter function is shown as the dotted line in Figure 6. The lower panels in Figure 6 show the "best estimate" CFRS luminosity function in the four redshift bins, $0.05 < z < 0.20$, $0.20 < z < 0.50$, $0.50 < z < 0.75$, and $0.75 < z < 1.0$ (as in Fig. 2*b* but now not split in color).

The most important point in Figure 6 is that the *differential* evolution of the blue luminosity function seen in Figures 2 and 5 relative to the static red luminosity function can produce effects on the *integrated* luminosity function that can be described as either a steepening of the faint end slope, α, or an increase in normalization, ϕ^*, if the color split is not made.

4.1. *The K-Band Selected Sample of Cowie et al. (1995)*

Cowie et al. (1995) have constructed a cumulative luminosity function from a set of *K*-selected samples of about 367 galaxies, including about 50 galaxies at $z > 0.5$. In broad terms, *K* selec-

tion and I selection should be more or less equivalent over the redshift range of interest since there is a relatively narrow range of $(I-K)_{AB}$ colors within the galaxy population. For instance, there is a variation of only about 1 mag between the $(I-K)_{AB}$ colors of the CWW E and Irr spectral energy distributions at $z = 0.8$. Figure 2 of Cowie et al. (1995) compares the cumulative luminosity function in a single $0.1 < z < 1$ bin with a local sample based extensively on the Mobasher, Sharples, & Ellis (1993) sample. This figure is thus most directly comparable with the upper panel in Figure 6 (although the median redshift of our sample is rather higher—0.56 as against 0.3). Cowie et al. note that the dominant effect in their sample must be a rise in the effective density ϕ^*, since the asymptotic luminosity density increases by a factor of 2.5 (for $q_0 = 0.5$) while the L^* remains almost constant. They conclude that individual galaxies were slightly fainter in the past (0.25 ± 0.2 mag) and that the number density rises as $(1+z)^{2.7}$. They infer that this requires that galaxies must be either combining through merging or else "disappearing" in some way as cosmic time progresses. They favored the first hypothesis because of the passive evolution that would have been expected to make galaxies brighter in the past, noting that the increase in luminosity of the *population* as a whole matched these evolutionary expectations, while the lack of increase in *individual objects* (i.e., in L^*) did not. The issues raised by passive evolution were discussed above in § 3.4.

From our own larger sample, however, it is clear that separating the population into red and blue components as on our Figure 2*b* shows that the apparent increase in ϕ^* comes about through the apparent brightening of the luminosity function of blue galaxies. This produces a large number of luminous blue galaxies with luminosities comparable to present-day L^*. Although the change in the population need not of course be produced by a corresponding evolution in individual objects, we note that quite modest changes to individual objects (1–2 mag of dimming over $0.5\tau_0$) are sufficient to account for the change in the population, especially if there is the low-luminosity population above the Loveday et al. (1992) luminosity function. The numerous blue galaxies seen at $z > 0.5$ do not need to "disappear" and can in fact fade by quite modest amounts to reproduce the observed effects. While we are thus unable to categorically rule out large-scale merging of galaxies, we do not believe that it is required.

4.2. *The B-Band Selected Sample of Colless (1995)*

Colless (1995) has constructed a preliminary luminosity function from the various B-selected samples extending down to the $22.5 < b_J < 24$ sample of Glazebrook et al. (1995). It is best defined at $z < 0.5$ since there are only 40 objects at $z > 0.5$. As in Broadhurst et al. (1988), the changes in this luminosity function have been described in terms of an increase in the faint end slope of the luminosity function. Qualitatively it shows similar behavior to the lower four panels of Figure 6. Perhaps of most interest in the present context is that in the B-selected samples analyzed by Colless (1995), the "excess" at low luminosities appears between $z \sim 0$ and $z \sim 0.2$ and is the cause of the original effect discussed by Broadhurst et al. (1988).

We address below (§ 5.2) the specific question of whether there is any observational inconsistency between the marked paucity of high-redshift galaxies at $z > 0.7$ in published B samples and the large number (33% of the sample) at these redshifts found in the I-band selected CFRS sample.

4.3. *The* Mg II *Absorption Sample of Steidel, Dickinson, & Persson (1994)*

Although small (58 objects at $0.3 < z < 1$, 70% with spectroscopically confirmed redshifts), the sample of Steidel et al. (1994) is particularly interesting because it is based on the galaxies producing Mg II λ2799 absorption lines in background quasars and thus represents a quite different selection methodology.

Steidel et al. (1994) concluded that neither the mean absolute magnitude nor the mean rest-frame $(B-K)$ color of the absorbing galaxies changes over this redshift interval $0.3 < z < 1.0$. The constancy of the mean color is at first sight surprising, given the changes in the CFRS population seen in Figures 3 and 5 above. It cannot be argued (cf. Steidel et al. 1994) that our evolving blue population simply has too low an absolute K magnitude to produce absorption lines, since all of the CFRS galaxies at $z > 0.5$ in fact have $M_{AB}(K) < -20$; i.e., they lie above the threshold for producing absorption lines in the Steidel et al. (1994) sample.

To study this question in more detail, we have plotted on Figure 7 the B-band absolute magnitudes (calculated for $q_0 = 0.5$) of the Steidel et al. (1994) absorbing sample as a function of redshift (using data kindly provided by Dr. Steidel). Following our analyses above, a linear regression of $M_{AB}(B)$ on z was separately computed for (1) the 28 red galaxies with rest $(B-K)_{AB} > 1.3$, (2) the 25 blue galaxies with rest $(B-K)_{AB} < 1.3$, and finally (3) for the subset of nine bluest galaxies with $(B-K)_{AB} < 1.0$. These lines are shown on Figure 7. While the absolute magnitudes of the red galaxies are indeed constant, the best fit to the two blue samples indicates an increase in the

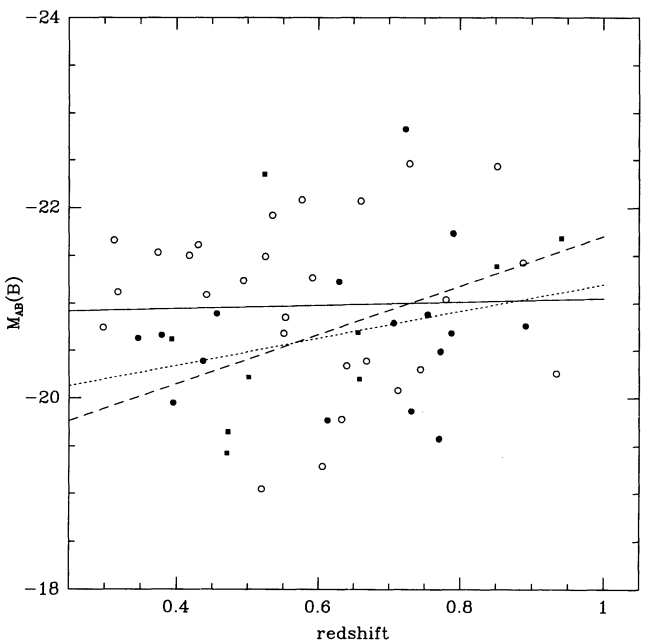

FIG. 7.—Variation in $M_{AB}(B)$ with redshift in the Steidel et al. (1995) sample of absorption-line selected galaxies, divided into redder galaxies (*open symbols*) and bluer galaxies (*filled symbols*). The bluest galaxies are represented by filled squares. The lines indicate linear regressions of $M_{AB}(B)$ on z for these three samples (red [*solid line*], bluer [*dotted line*], and bluest [*dashed line*]). Although of marginal significance in this small sample, the constancy in the luminosity of red galaxies and the increase in the luminosity of bluer galaxies is as found in the present work.

average luminosity between $0.3 < z < 1.0$ of 1 mag for the blue sample and 2 mag for the very bluest objects.

Although these effects are of marginal significance in the small Steidel et al. (1994) sample, they are entirely consistent with the changes seen on our Figures 2 and 5 above. It is clear on Figure 7 that the color-magnitude relation, which is clearly apparent in the absorbing sample at $z < 0.5$, breaks down at higher redshifts, exactly as seen in our Figure 5. We thus believe that, at present, the two samples are entirely consistent.

5. $N(z)$ AND COUNT EXTRAPOLATIONS TO FAINTER MAGNITUDES AND FOR OTHER WAVE BANDS

The V_{max} approach to calculating the luminosity can be easily modified to produce predictions for the counts and redshift distributions at fainter magnitudes and in different wave bands. As described in LCG, for each galaxy observed in our own sample for which a V_{max} was calculated as above, the apparent magnitude as a function of redshift (placing the galaxy at all redshifts $0 < z < \infty$) is calculated in any wave band of interest from the known absolute magnitude and rest-frame spectral energy distribution. The contribution to the counts and/or $N(z)$ distribution at this apparent magnitude is then simply dV/dz divided by the V_{max} obtained as above for the galaxy in our I-band sample. This analysis is thus based on the implicit assumption that the observed population in our $17.5 < I_{AB} < 22.5$ sample does not evolve at either higher or lower redshifts. For simplicity we use the "best estimate" sample for this exercise.

The number counts in the B band and I band that are generated in this way from the CFRS sample are shown in Figure 8 compared with number counts from the literature (taken from LCG and references therein—see Koo & Kron 1992 for a review). In the next section we discuss the I-band extrapolation and then turn to the B-band extrapolation.

5.1. *Extrapolation in the I Band*

By definition, the CFRS-based no-evolution prediction must match well the I-band counts around $I_{AB} \sim 22$, and the small discrepancy at this magnitude arises purely from the fact that stars are excluded from the prediction but are included in the deep counts. As discussed by LCG, the flatter slope at brighter magnitudes is simply a reflection of the evolution already observed in the sample (e.g., Figs. 2*a*–2*c*)—the sample contains high-redshift objects at $z > 0.5$ that are not present at low redshift. At fainter magnitudes, the extrapolated counts fall below the observed counts, which implies that there is continuing evolution of some sort to fainter magnitudes. At $I_{AB} \sim 24$ (2 mag below the CFRS), the observed count is 1.6 times that predicted from replicating the observed CFRS population to higher redshifts without any evolution.

The modest shortfall at fainter magnitudes suggests that the predicted $N(z)$ from this model may be quite useful in estimating the redshift distributions of very faint I-band selected galaxies that lie beyond the reach of current spectrographs. Topical studies in this area include measurements of the small distortions of background galaxies by intervening mass concentrations (e.g., Kaiser & Squires 1993) and the interpretation of the morphologies of the faintest galaxies revealed on very deep *Hubble Space Telescope* images. We show in Figure 9 the $N(z)$ predicted from this analysis for the $17.5 < I_{AB} < 22.5$ range of the CFRS and two fainter 1 mag slices of I_{AB}.

5.2. *Extrapolation in the B Band*

In the B band, the shortfall at fainter magnitudes is more severe (see Fig. 8). Indeed, even at $B \sim 24$, there is already a

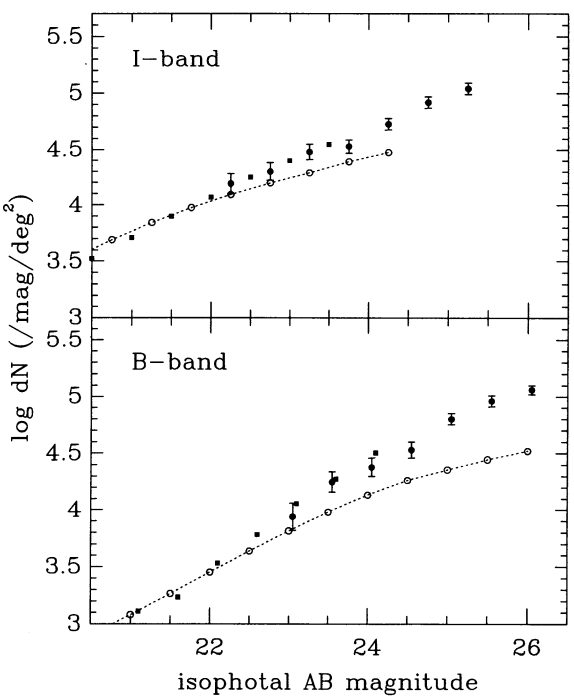

FIG. 8.—Number magnitude counts in the I band and B band obtained by replicating the observed CFRS population to higher redshifts (*connected open symbols*), compared with observations (taken from LCG; *filled symbols*). There is a modest shortfall in the I band but a substantial one in the B band, which indicates further evolution in the luminosity function from blue galaxies will be required.

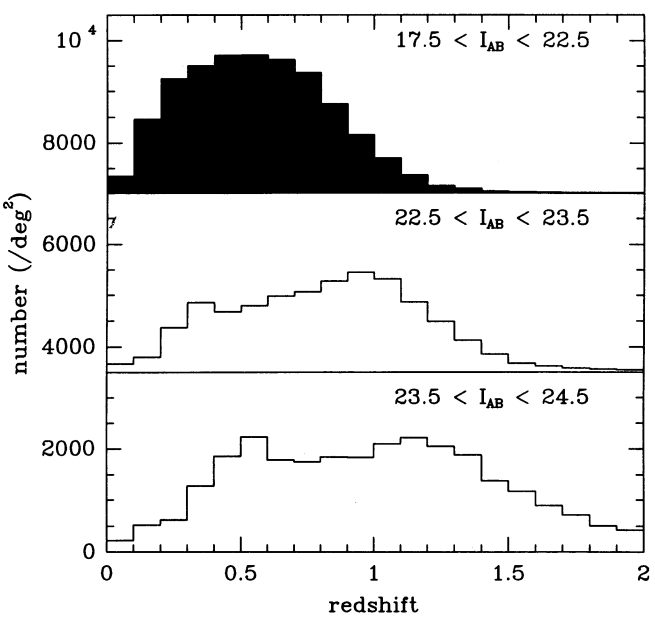

FIG. 9.—The $N(z)$ distributions obtained from the CFRS luminosity function in the $17.5 < I_{AB} < 22.5$ range (*upper histogram*) and extrapolated, assuming no further evolution, to fainter magnitudes, $22.5 < I_{AB} < 23.5$ and $23.5 < I_{AB} < 24.5$.

shortfall of around 30%. This implies that a $B < 24$ sample contains a number of very blue galaxies that are not represented in the $I_{AB} < 22.5$ selected CFRS. This should not be surprising because, as shown in LCG, the median $(B-I)_{AB}$ colors fall sharply, by at least 0.5 mag, between $I_{AB} = 22.5$ and $I_{AB} = 24.5$, which implies a rapid increase in the relative numbers of very blue galaxies with increasing depth in the B-selected samples. A slightly deeper I-band sample would contain many more of these very blue galaxies that would have $B \sim 24$. We return to this point below. At the faintest magnitudes there is a shortfall of a factor of 3, and any $N(z)$ generated from this analysis is of limited use.

At this stage, we can only speculate on the nature of the evolving population that fills in the steep number counts. Given what we have seen in the evolution of the bright blue galaxies, it may well be that these very faint objects will turn out to be at moderate redshifts and to represent the faint end of the luminosity functions shown in Figure 2*b*.

One of the more interesting aspects of the $N(z)$ distributions from B-selected samples has been the marked paucity of galaxies at $z > 0.7$. The combined $21 < b_J < 22.5$ sample of Colless et al. (1990, 1993) has 4% of galaxies at $z > 0.7$ with an unidentified fraction of only 6%, while the deeper $22.5 < b_J < 24$ sample of Glazebrook et al. (1995) has 13% with a much larger 30% unidentified fraction. In contrast the I-band selected CFRS sample has approximately 33% of galaxies at $z > 0.7$. The $22.5 < B < 24$ sample of Cowie et al. (1991) has only 12 objects, of which one has $z > 0.7$ (L. Cowie, private communication), although there are two more with $0.65 < z < 0.7$.

The Colless et al. (1990, 1993) samples are sufficiently bright that we can directly construct an equivalent sample from the CFRS $17.5 < I_{AB} < 22.5$ sample [since virtually no objects have $(b_J - I_{AB}) < 0$] at least in the three fields for which we have B photometry. This $21 < b_J < 22.5$ subsample of the CFRS contains 95 galaxies of which we have secure identifications for all but three (i.e., a 97% completeness). Seven galaxies have $z > 0.7$ (7%), which indicates no significant observational inconsistency at this level.

In order to assess the situation at the fainter levels, we used the V_{max} formalism described above to predict $N(z)$ distributions for a $22.5 < B < 24$ sample. It should be stressed that the analysis presented here should account for the different visibility of different classes of objects in the different wave bands but does not incorporate any evolutionary effects with redshift. With this caveat in mind, the fraction of galaxies predicted at $z > 0.7$ for $22.5 < B < 24$ is 30%, considerably higher than seen hitherto in the B samples at this depth. However, it should be noted that there is a large fraction of unidentified objects (30%) in the full Glazebrook et al. (1995) sample (a subset of 30 objects has only 10% unidentified). The explanation probably lies in a combination of effects. The very blue galaxies that are present in a $B < 24$ sample but are absent from the $I_{AB} < 22.5$ CFRS may well be at relatively low redshifts, and, if this is the case, this will decrease the fraction of high-redshift galaxies. Furthermore, the fraction of galaxies expected at $z > 0.7$ is increasing rapidly with depth. As discussed in CFRS I, our faint isophotal level for photometry ensures that even for these faint objects, we include nearly all of the light, whereas other photometry schemes may miss the equivalent of a few tenths of a magnitude. Perhaps the most likely explanation is that the existing B-selected samples may be systematically missing the high-redshift objects, perhaps because of limited spectral range.

We are currently extending the CFRS survey by observing blue objects so as to allow the direct construction of deeper B-selected samples. The results of this will be reported elsewhere.

6. SUMMARY

The cosmic evolution of the field galaxy population has been studied over the redshift interval $0 < z < 1.3$ using the 730 galaxies (median $\langle z \rangle \sim 0.56$) in the I-band selected CFRS redshift survey. The evolution of the population is best defined in terms of the trivariate luminosity function $\phi(M, \text{color}, z)$. The sample is large enough and spans a wide enough range in redshift and look-back time that evolutionary effects can be seen within the sample, thereby eliminating reliance on knowledge of the local population.

Three results have been found that indicate strongly differential evolution within the galaxy population.

1. The luminosity function of red galaxies (defined as redder than a typical present-day Sbc galaxy) shows very little change in either number density or luminosity over the entire redshift range $0 < z < 1$, an interval corresponding to the last $\frac{2}{3}$ of the age of the universe (for $\Omega \sim 1$). The luminosity function of the red galaxies is consistent with no change at all with z. Between $z \sim 0.8$ and $z \sim 0.3$, a change in luminosity of at most a few tenths of a magnitude and a change in density of at most 33% is indicated.
2. The luminosity function of blue galaxies (i.e., bluer than the present-day Sbc) shows substantial evolution at redshifts $z > 0.5$. At $0.2 < z < 0.5$, these galaxies are concentrated at low luminosities. By $0.5 < z < 0.75$ the population appears to have uniformly brightened by approximately 1 mag (although this could also be described as an increase in comoving density). At higher redshifts, the evolution appears to saturate at the brightest magnitudes but continues at fainter levels, which leads to a steepening of the luminosity function. At the highest redshifts $1.0 < z < 1.3$, we sample only the bright end of the luminosity function, and no additional evolution is seen.
3. At low redshifts $z < 0.2$, a significant excess relative to the Loveday et al. (1992) local luminosity function is seen around $M_{AB}(B) \sim -18$, similar to (though slightly brighter than) that found by Marzke et al. (1994a) in the local CfA survey. Our color-dependent local luminosity function is very similar to that of Metcalfe et al. (1991) and qualitatively similar to that of Marzke et al. (1994b). This numerous population, which may have evolved since $z \sim 0$, may represent the descendants for the evolving blue population seen at higher redshifts after modest luminosity evolution. This population would remove some of the motivations for introducing an exotic population to account for the numerous blue population seen at $z > 0.5$.

The changes seen in the luminosity function are also apparent in color-magnitude diagrams constructed at different epochs and in the V/V_{max} statistic computed as a function of spectral type. Given that the evolution is seen within a single sample, we regard this as secure evidence for changes in the galaxy population and believe that the no-evolution hypothesis (e.g., Koo et al. 1993) is no longer tenable.

It is argued that the picture of galaxy evolution presented here presents no inconsistencies with the very much smaller samples of field galaxies that have been selected in other wave bands (B and K), or with the results of studies of galaxies selected on the basis of Mg II λ2799 absorption

The CFRS project would not have been possible without the support of the directors of CFHT and of our two national TACs (CTAC and CFGT). We have benefited during the course of this project from conversations with many colleagues and particularly Ray Carlberg, Richard Ellis, Chuck Steidel, Mike Fall, and Len Cowie. We are also grateful to the referee for his careful reading of the manuscript. Chuck Steidel kindly provided his data to us in electronic form. S. J. L.'s research is supported by the NSERC of Canada, and the project has been facilitated by a travel grant from NATO.

REFERENCES

Babul, A., & Rees, M. J. 1992, MNRAS, 255, 346
Broadhurst, T. J., Ellis, R. S., & Glazebrook, K. 1992, Nature, 355, 55
Broadhurst, T. J., Ellis, R. S., & Shanks, T. 1988, MNRAS, 235, 827
Bruzual A., G. 1983, ApJS, 53, 497
Bruzual A., G., & Charlot, S. 1993, ApJ, 405, 538
Coleman, G. D., Wu, C. C., & Weedman, D. W. 1980, ApJS, 43, 393 (CWW)
Colless, M. 1995, in Wide Field Spectroscopy and the Distant Universe, Proc. 35th Herstmonceux Conference, ed. S. Maddox (Singapore: World Scientific), in press
Colless, M., Ellis, R., Broadhurst, T., Taylor, K., & Peterson, B. 1993, MNRAS, 261, 19
Colless, M. M., Ellis, R. S., Taylor, K., & Hook, R. N. 1990, MNRAS, 244, 408
Cowie, L. L., Songaila, A., & Hu, E. M. 1991, Nature, 354, 460
———.1995, preprint
Crampton, D., Le Fèvre, O., Lilly, S. J., & Hammer, F. 1995, ApJ, 455, 96 (CFRS V)
Dressler, A., Gunn, J. E., & Schneider, D. 1985, AJ, 294, 70
Eales, S. A. 1993, ApJ, 404, 51
Felten, J. E. 1976, ApJ, 207, 700
Ferguson, H., & McGaugh, S. 1995, ApJ, 440, 470
Glazebrook, K., Ellis, R. S., Colless, M. M., Broadhurst, T. J., Allington-Smith, J. R., Tamvir, N. R., & Taylor, K. 1995, MNRAS, in press
Hammer, F., Crampton, D., Le Fèvre, O., & Lilly, S. J. 1995, ApJ, 455, 88 (CFRS IV)
Hudon, J. D., & Lilly, S. J. 1996, ApJ, submitted
Kaiser, N., & Squires, G. 1993, ApJ, 404, 441
Koo, D. C. 1986, ApJ, 311, 651
Koo, D. C., Gronwall, C., & Bruzual A., G. 1993, ApJ, 415, L21
Koo, D. C., & Kron R. G. 1992, ARA&A, 30, 613
Kron, R. G. 1980, ApJS, 43, 305
Le Fèvre, O., Crampton, D., Lilly, S. J., Hammer, F., & Tresse, L. 1995, ApJ, 455, 60 (CFRS II)
Le Fèvre, O., Hudon, D., Lilly, S. J., Crampton, D., & Hammer, F. 1996, ApJ, submitted (CFRS VIII)
Lilly, S. J. 1993, ApJ, 411, 501
Lilly, S. J., Cowie, L. L., & Gardner, J. P. 1991, ApJ, 369, 79 (LCG)
Lilly, S. J., Hammer, F., Le Fèvre, O., & Crampton, D. 1995a, ApJ, 455, 75 (CFRS III)
Lilly, S. J., Le Fèvre, O., Crampton, D., Hammer, F., & Tresse, L. 1995b, ApJ, 455, 50 (CFRS I)
Loh, E., & Spillar, E. J. 1986, ApJ, 307, L1
Lonsdale, C. J., & Chokshi, A. 1993, AJ, 105, 1333
Loveday, J., Peterson, B. A., Efstathiou, G., & Maddox, S. J. 1992, ApJ, 390, 338
Marzke, R. O., Geller, M. J., Huchra, J. P., & Corwin, H. 1994a, ApJ, 428, 43
———. 1994b, AJ, 108, 437
Metcalfe, N., Shanks, T., Fong, R., & Jones, L. R. 1991, MNRAS, 249, 498
Mobasher, B., Sharples, R. M., & Ellis, R. S. 1993, MNRAS, 263, 560
Oke, J. B. 1972, ApJS, 27, 21
Rakos, K. D., & Schombert, J. M. 1995, ApJ, 439, 47
Schade, D. J., Lilly, S. J., Crampton, D., Hammer, F., Le Fèvre, O., & Tresse, L. 1995, ApJ, 451, L1 (CFRS IX)
Schmidt, M. 1968, ApJ, 151, 343
Songaila, A., Cowie, L. L., Hu, E. M., & Gardner, J. P. 1994, ApJS, 94, 461
Steidel, C., Dickinson, M. J., & Persson, S. E. 1994, ApJ, 437, L75
Tinsley, B. M., & Gunn, J. E. 1976, ApJ, 203, 52
Tresse, L., Hammer, F., Le Fèvre, O., & Proust, D. 1993, A&A, 277, 53
Yoshii, Y., & Fukugita, M. 1992, in Observational Tests of Cosmological Inflation, ed. T. Shanks, A. J. Barclay, R. S. Ellis, C. S. Frenk, & A. N. Wolfendale (Dordrecht: Kluwer), 267
Yoshii, Y., & Takahara, F. 1988, ApJ 326, 1